doi:10.1016/j.jmb.2010.02.034 J. Mol. Biol. (2010) 398, 320–331

JMB

Available online at www.sciencedirect.com

ScienceDirect

ELSEVIER

Disulfide-Reduced ALS Variants of Cu, Zn Superoxide Dismutase Exhibit Increased Populations of Unfolded Species

Can Kayatekin†, Jill A. Zitzewitz‡ and C. Robert Matthews*

Department of Biochemistry and Molecular Pharmacology, University of Massachusetts Medical School, Worcester, MA 01605, USA

Received 13 November 2009; received in revised form 15 February 2010; accepted 17 February 2010
Available online 23 February 2010

Cu,Zn superoxide dismutase (SOD1) is a dimeric metal-binding enzyme responsible for the dismutation of toxic superoxide to hydrogen peroxide and oxygen in cells. Mutations at dozens of sites in SOD1 induce amyotrophic lateral sclerosis (ALS), a fatal gain-of-function neurodegenerative disease whose molecular basis is unknown. To obtain insights into effects of the mutations on the folded and unfolded populations of immature monomeric forms whose aggregation or self-association may be responsible for ALS, the thermodynamic and kinetic folding properties of a set of disulfide-reduced and disulfide-oxidized Zn-free and Zn-bound stable monomeric SOD1 variants were compared to properties of the wild-type (WT) protein. The most striking effect of the mutations on the monomer stability was observed for the disulfide-reduced metal-free variants. Whereas the WT and S134N monomers are >95% folded at neutral pH and 37 °C, A4V, L38V, G93A, and L106V ranged from 50% to ~90% unfolded. The reduction of the disulfide bond was also found to reduce the apparent Zn affinity of the WT monomer by 750-fold, into the nanomolar range, where it may be unable to compete for free Zn in the cell. With the exception of the S134N metal-binding variant, the Zn affinity of disulfide-oxidized SOD1 monomers showed little sensitivity to amino acid replacements. These results suggest a model for SOD1 aggregation where the constant synthesis of ALS variants of SOD1 on ribosomes provides a pool of species in which the increased population of the unfolded state may favor aggregation over productive folding to the native dimeric state.

Edited by P. Wright

Keywords: disulfide bond; Zn binding; protein folding; aggregation

Introduction

Amyotrophic lateral sclerosis (ALS) is a fatal neurodegenerative disease that results in the death of motor neurons.[1] An inherited form of ALS has been linked to mutations in the gene encoding for the Cu,Zn superoxide dismutase (SOD1).[2,3] To date, more than 150 amino acid replacements, insertions, deletions, and truncations throughout the sequence have been discovered that give rise to this deleterious gain-of-function disease§.[4] Although a number of mechanisms have been proposed for toxicity,[5] ALS variants of SOD1 often lead to the formation of macroscopic aggregates in the motor neurons of afflicted individuals. Recognizing that these types of sequence alterations typically destabilize proteins, it is reasonable to hypothesize that marginally soluble forms of SOD1 self-associate to produce toxic small oligomers or larger aggregates.[6] Nevertheless, the conformations of SOD1 responsible for aggregation are unclear, and a common molecular explanation for the formation of these aggregates has not been discovered.

*Corresponding author. Department of Biochemistry and Molecular Pharmacology, University of Massachusetts Medical School, 364 Plantation Street, LRB 927, Worcester, MA 01605, USA. Fax: +1 508-856-8358. E-mail address: C.Robert.Matthews@umassmed.edu.

† Can.Kayatekin@umassmed.edu.

‡ Jill.Zitzewitz@umassmed.edu.

Abbreviations used: ALS, amyotrophic lateral sclerosis; EDTA, ethylenediaminetetraacetic acid; Gdn-HCl, guanidine hydrochloride; mAS-SOD1, F50E/G51E/C6A/C11S monomeric variant of SOD1; SOD1, human Cu,Zn superoxide dismutase; TCEP, tris(2-carboxyethyl) phosphine.

§ http://alsod.iop.kcl.ac.uk/Als/Index.aspx

SOD1 is a cytosolic protein responsible for the dismutation of superoxide, a toxic byproduct of metabolism, into hydrogen peroxide and oxygen through the cyclical oxidation and reduction of its catalytic Cu ion.[7] In its mature form, SOD1 is a homodimer with one Zn and one Cu ion bound to each subunit. The fold of each monomer can be described as a β-sandwich composed of eight β-strands supporting two large loops. The Zn-binding loop binds the structurally important Zn ion, and the electrostatic loop plays a role in guiding the superoxide anion to the active site. In addition, each monomer contains an intramolecular disulfide bond between C57 in the Zn-binding loop and C146 in β8 (Fig. 1).

There has been growing interest in the role of immature monomeric species, that is, metal free and/or disulfide reduced, in aggregation.[8] Monomeric species of SOD1 may be more prone to aggregation[9–11] because they are likely to be partially folded and marginally soluble.[12–15] This hypothesis is consistent with the three-state folding mechanism of SOD1, $2U \leftrightarrows 2M \leftrightarrows N_2$, in which the rate-limiting monomer folding reaction from the unfolded state, U, to the folded state, M, is followed by the rapid association of the monomers to form the dimeric native state, N_2.[16,17] As a consequence, the folded monomer population is minimized during the folding reaction of the wild-type (WT) protein. Also supporting this view is the observation that several ALS variants destabilize the native state, leading to increased populations of folded and unfolded monomeric species at equilibrium.[18–20] These studies focused on forms of SOD1 and its variants that contain the intramolecular disulfide bond, in essence, the mature species closely connected with the native conformation.

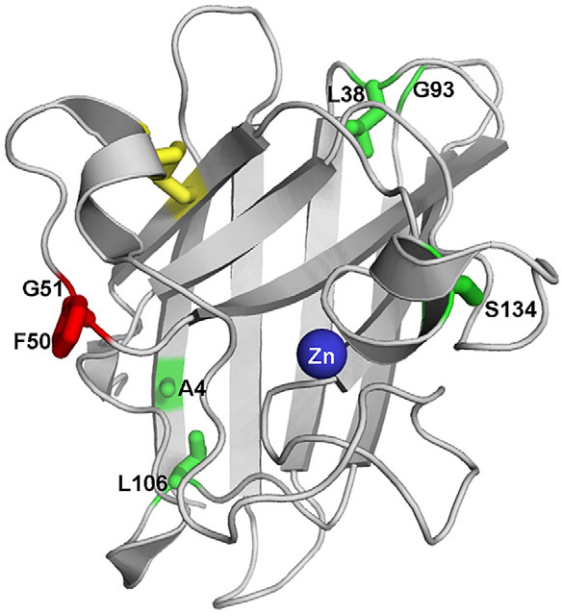

Fig. 1. Crystal structure of holo-SOD1 (PDB: 2C9V). The Cu ion and the other monomer have been omitted. The disulfide bond is highlighted in yellow, and the Zn ion in blue. The sites of ALS mutations studied are highlighted by the green side chains for the native amino acids. The two residues replaced by glutamic acid to create the monomer model, F50 and G51, are shown in red. The ALS-inducing variants studied are A4V, L38V, G93A, L106V, and S134N.

It has previously been shown that the reduction of the disulfide bond leads to the dissociation of the dimer in the absence of metal ions; zinc binding reverses this process.[21] The reduction of the disulfide bond in several ALS-inducing variants decreases the apparent melting point below physiological temperature.[22] However, the irreversibility of the thermal unfolding reaction and the requirement for a stabilizing osmolyte render this conclusion ambiguous. To obtain unambiguous quantitative insight into the thermodynamic coupling between disulfide bond, Zn binding, and amino acid replacements on immature SOD1, a combined thermodynamic and kinetic analysis of the reversible folding reactions of a monomeric version of SOD1 (mAS-SOD1), C6A/F50E/G51E/C111S, and five ALS variants introduced into this background (Fig. 1) was performed. The A4V mutation increases the side-chain volume in a tightly packed hydrophobic cluster inside the β-sandwich. Both L38 and L106 serve as hydrophobic capping residues for the β-sandwich, and replacement with valine at these positions decreases the side-chain volume and replaces a γ-branched side chain with a β-branched side chain. The main chain of G93 is in a tight loop, and the dihedral angles are disfavored for all but glycine at this position. Finally, S134 is involved in the hydrogen-bonding network that links the electrostatic loop to the Zn-binding loop, and its replacement with asparagine leads to decreased metallation (for a general review, see Valentine *et al.*[5]).

With the exception of S134N, both oxidized and reduced monomeric forms of the remaining variants exhibited a significant loss of thermodynamic stability for their metal-free forms. By contrast, S134N was the only variant studied that exhibited a significantly weakened apparent Zn affinity. Surprisingly, the reduction of the disulfide bond decreased the affinity of WT mAS-SOD1 for Zn by ~750-fold. The substantially increased populations of the unfolded forms in four of the five disulfide-reduced ALS variants of SOD1 at physiological temperature may provide the common link between mutations at many positions and protein aggregation. The reduction in the apparent Zn affinity of the S134N variant would allow this variant to more readily sample the metal-free folding free-energy surface whose folded and/or unfolded monomeric populations might be sufficient to induce aggregation even for WT SOD1.

Results

The thermodynamic stability of the Zn-bound and/or disulfide-reduced states of monomeric WT, A4V, L38V, G93A, L106V, and S134N SOD1 variants

was determined by chemical denaturation experiments on the C6A/F50E/G51E/C111S model of SOD1 (Fig. 1).[23] In this pseudo-WT model, the free cysteines, C6 and C111, have been replaced with nonoxidizable side chains to eliminate intramolecular disulfide interchange in the unfolded state and intermolecular disulfide cross-linking in the native state. The F50 and G51 residues at the dimer interface have been replaced with glutamic acid to prevent dimerization.[24,25] The structure of this stable monomer is very similar to that for the monomer in the context of the dimer,[25,26] as is the thermodynamic stability.[17] This system enables measurements of highly reversible folding reactions solely for the monomeric forms of these ALS variants, in the absence of their self-association to dimeric species. Although the C6A/C111S and F50E/G51E mutations might themselves perturb the aggregation propensity of SOD1 (C6F, C6G, and C111Y are ALS variants[8]), the introduction of ALS-inducing mutations into the same background allows for a direct comparison of their perturbations

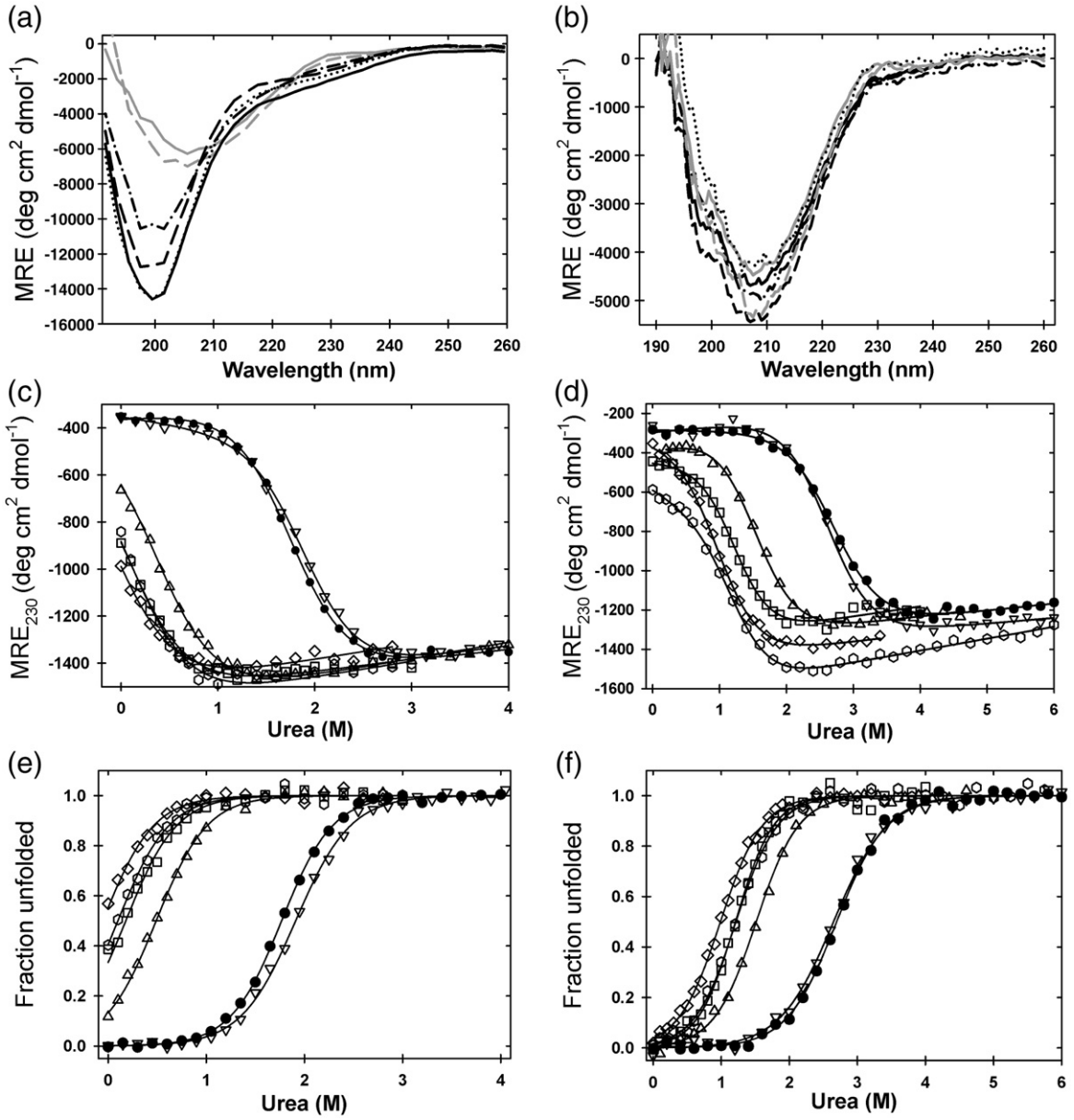

Fig. 2. CD spectra and urea titrations reveal that A4V, L38V, G93A, and L106V mAS-SOD1$^{2SH}_{Apo}$ are partially unfolded. The CD spectra of WT (solid gray), A4V (dash-dot black), L38V (dotted black), G93A (dashed black), L106V (solid black), S134N (dashed gray) (a) mAS-SOD1$^{2SH}_{Apo}$ and (b) mAS-SOD1$^{SS}_{Apo}$ at 20 °C and pH 7.2. Equilibrium unfolding curves at 20 °C and pH 7.2 for (c) mAS-SOD1$^{2SH}_{Apo}$ and (d) mAS-SOD1$^{SS}_{Apo}$ variants and the calculated fraction unfolded plots for (e) mAS-SOD1$^{2SH}_{Apo}$ and (f) mAS-SOD1$^{SS}_{Apo}$ variants measured by CD at 230 nm: WT (filled circle), A4V (triangle), L38V (hexagon), G93A (diamond), L106V (square), S134N (upside-down triangle). Best-fit curves to a two-state U ⇆ M folding model are shown in continuous lines. The thermodynamic data are presented in Table 1. The protein concentration for these experiments was 10 μM.

on the thermodynamic properties and populations of the SOD1 system.

Stabilities of disulfide-reduced apo-mAS-SOD1

The role of the disulfide bond in stabilizing mAS-SOD1$_{Apo}$ was determined by reducing the disulfide bond and monitoring the ellipticity at pH 7.2 and 20 °C as a function of the urea concentration. The choice of urea as the denaturant was necessitated by the expected low thermodynamic stability of these proteins. The far-UV circular dichroism (CD) spectra of the disulfide-reduced monomers can be seen in Fig. 2a. WT and S134N mAS-SOD1Apo exhibit a minimum at ~208 nm and a slight shoulder at 230 nm, consistent with a significant degree of folding. In contrast, A4V, L38V, G93A, and L106V mAS-SOD1Apo exhibit unfolded-like CD spectra with the minimum shifted to ~200 nm, and they lack the shoulder at 230 nm characteristic of the native fold.

The equilibrium urea denaturation curves for mAS-SOD1Apo variants are shown in Fig. 2c. WT mAS-SOD1Apo is stable to ~1.2 M urea, where it undergoes a cooperative unfolding reaction that is complete by ~2.6 M urea. The S134N variant is nearly coincident with WT with the exception of a slightly negatively sloped native baseline prior to the cooperative unfolding transition. The A4V, L38V, G93A, and L106V variants are all completely denatured by 1 M urea and lack native baselines. These equilibrium data were fit to a two-state model, U ⇆ M, assuming a linear dependence of the apparent free energy of folding, $\Delta G°$, on the denaturant concentration: $\Delta G°$ (urea) = $\Delta G°$ (H_2O) − m[urea] (Table 1). All data were fit using Savuka 6.2, an in-house nonlinear least-squares program using the Marquardt–Levenberg algorithm. The fits were performed by globally analyzing the ellipticity at 20 different wavelengths between 220 and 240 nm. Both WT and S134N mAS-SOD1Apo exhibit well-defined baselines and were fit without constraining the parameters. From the determined thermodynamic stability (Table 1), it is evident that both of these proteins are >99% folded under these conditions (Fig. 2e). For the highly destabilized ALS variants where no native baseline was observed, the m value and the slope and intercept of the native baseline were fixed to the same values as that of WT. The constraint on several variables, required to fit these titrations, likely results in an underestimated error of the fit, suggesting caution in the accuracy of these estimates for stability. Nevertheless, the lack of native baselines and the reduced CD signal in the absence of denaturant (Fig. 2b) make it clear that substantial fractions of A4V, L38V, G93A, and L106V mAS-SOD1Apo are unfolded at 20 °C and pH 7.2 (Fig. 2e).

The large fraction of unfolded protein for the A4V, L38V, G93A, and L106V variants at 20 °C and the known endothermic unfolding reaction for SOD1[27] prompted a comparison of the urea denaturation

Table 1. Thermodynamic parameters, microscopic rate constants, and kinetic $m^{‡}$ values for monomeric variants

	WT	A4V	L38V	G93A	L106V	S134N
Apo reduced[a]						
$\Delta G°_{(U/M)}$[b]	−3.95±0.1	−1.09[c]	−0.22[c]	+0.12[c]	−0.40[c]	−3.97±0.16
$m_{(U/M)}$	2.23±0.11	2.23[d]	2.23[d]	2.23[d]	2.23[d]	2.08±0.08
Apo oxidized[a,e]						
$\Delta G°_{(U/M)}$[b]	−4.48±0.07	−2.83±0.07	−2.32±0.15	−1.87±0.07	−2.52±0.08	−4.54±0.10
$m_{(U/M)}$	1.65±0.02	1.88±0.04	1.91±0.08	1.89±0.04	2.09±0.05	1.73±0.03
Apo oxidized[a,e]						
k_f	0.056±0.002	0.15±0.02	0.033±0.006	0.029±0.004	0.030±0.003	0.039±0.004
$m_f^{‡}$	1.20±0.05	1.5±0.1	1.36±0.20	1.37±0.18	1.33±0.13	1.13±0.04
k_u	(2.02±0.40)×10^{-5}	(1.0±0.1)×10^{-3}	(3.5±1.5)×10^{-4}	(1.2±0.2)×10^{-3}	(5.0±1.0)×10^{-4}	(1.2±0.1)×10^{-5}
$m_u^{‡}$	−0.58±0.01	−0.64±0.03	−0.78±0.09	−0.74±0.03	−0.74±0.05	−0.65±0.01
$\Delta G°_{(U/M)}$	−4.61±0.12	−2.92±0.2	−2.65±0.28	−1.85±0.13	−2.37±0.13	−4.70±0.08
$m_{(U/M)}$[f]	1.79±0.05	2.14±0.1	2.14±0.22	2.11±0.18	2.07±0.14	1.78±0.04
Zn oxidized[g]						
k_f	0.74±0.01	0.87±0.15	0.27±0.05	0.19±0.05	0.34±0.05	0.64±0.01
$m_f^{‡}$	2.93±0.07	3.0±0.1	2.89±0.09	2.48±0.17	3.39±0.10	2.95±0.10
k_u	(0.23±0.08)×10^{-7}	(1.77±0.39)×10^{-7}	(2.8±0.8)×10^{-7}	(4.1±1.2)×10^{-7}	(13.3±3.9)×10^{-7}	(2.8±1.2)×10^{-7}
$m_u^{‡}$	−1.76±0.05	−1.85±0.03	−2.01±0.06	−1.88±0.06	−1.68±0.06	−1.47±0.13
$\Delta G°_{(U/M)}$[h]	−18.0±0.2	−17.0±0.2	−15.3±0.5	−15.6±0.2	−15.2±0.2	−16.5±0.3
$m_{(U/M)}$[f]	4.69±0.09	4.85±0.1	4.90±0.11	4.36±0.18	5.07±0.12	4.42±0.13
$\Delta G°_{Zn}$	−13.4±0.2	−14.1±0.2	−12.7±0.5	−13.8±0.2	−12.8±0.2	−11.8±0.3
K_d[h] (pM)	100±39	31±15	360±350	55±23	270±110	1600±840

Units for the U ⇆ M reaction: k_f and k_u, s^{-1}; $m_f^{‡}$, $m_u^{‡}$, and $m_{(U/M)}$, kcal mol^{-1} M^{-1}; $\Delta G°_{(U/M)}$, $\Delta G°_{Zn}$, kcal mol^{-1}.

[a] Denaturation was performed with urea.

[b] Equilibrium data were fit to a two-state model, U ⇆ M, by globally analyzing the CD signal at 20 different wavelengths between 220 and 240 nm.

[c] Due to the constraints required to fit these titrations, the error in the free energy of folding is approximated to be ±0.3 kcal mol^{-1}.

[d] The parameter was fixed to the WT value.

[e] WT values adapted from Svensson *et al.*[16]

[f] Calculated according to the equation $m_{tot} = /m_u^{‡}/ + /m_f^{‡}/$.

[g] Denaturation was performed with Gdn-HCl.

[h] The free-energy difference between U + Zn ⇆ N•Zn and the Zn affinity was calculated as described in Kayatekin *et al.*[30]

reactions for WT and A4V mAS-SOD1Apo over the temperature range from 4 to 37 °C to determine the extent of unfolding at physiological temperature, 37 °C. While the stability of WT protein can be measured reliably at 37 °C, A4V is too destabilized at these temperatures to allow accurate fitting of the data. For both A4V and WT, the thermodynamic stability was determined by a singular value decomposition analysis of CD spectra from 220 to 240 nm.[28] The singular value decomposition vectors were normalized to the unfolded baseline and fit by holding the slope and *y*-intercept of the native baseline fixed to the 4 °C data set. A van't Hoff plot of the results is shown in Fig. 3. The data are well described by a simple linear dependence whose calculated enthalpy changes, 23.8±2.8 kcal mol^{-1} for WT and 20.3±2.2 kcal mol^{-1} for A4V, allow for the prediction of the stabilities at 37 °C.

The stability of WT mAS-SOD1Apo is 2.0 kcal mol^{-1} at pH 7.2 and 37 °C, meaning that ~97% of the protein is folded under these conditions. By contrast, the stability of A4V mAS-SOD1Apo, which could be measured reliably up to 27 °C, falls from 2.1 kcal mol^{-1} at 4 °C to 0.8 kcal mol^{-1} at 27 °C. Linear extrapolation to 37 °C reveals that the stability is reduced to ~0 kcal mol^{-1}, indicating that A4V is half unfolded under physiological conditions. These results are consistent with previous native-state hydrogen-exchange experiments that showed WT SOD1Apo retained some protection against amide hydrogen exchange at 37 °C, while A4V SOD1Apo did not.[29] Urea titrations at 37 °C for all variants can be seen in Fig. 4. For the highly destabilized variants, these titration curves entirely lack native baselines and display a very small portion of the unfolding transition, consistent with the conclusion that these proteins are largely unfolded at 37 °C. On the other hand, the S134N and WT variants are nearly indistinguishable and appear reasonably well folded under these conditions.

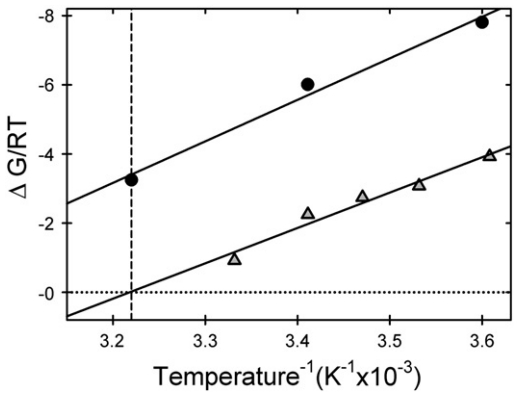

Fig. 3. The van't Hoff plot of WT (circle) and A4V (triangle) mAS-SOD1$^{2SH}_{Apo}$. The stability at each temperature was determined from a urea titration. Linear extrapolations to physiological temperature are shown by the continuous black lines. The black, dashed, vertical line indicates 37 °C, while the dashed line represents a folding free energy of zero, where the protein is half unfolded. The buffer used was 20 mM Hepes, 1 mM EDTA, 1 mM TCEP (pH 7.2).

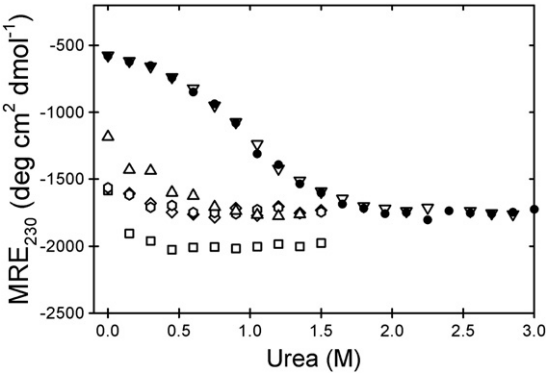

Fig. 4. Equilibrium unfolding curves at 37 °C and pH 7.2 for WT mAS-SOD1$^{2SH}_{Apo}$ and ALS variants as measured by CD at 230 nm: WT (filled circle), A4V (triangle), L38V (hexagon), G93A (diamond), L106V (square), S134N (upside-down triangle). The buffer used was 20 mM Hepes, 1 mM EDTA, 1 mM TCEP (pH 7.2).

Stabilities of disulfide-oxidized apo-mAS-SOD1

The far-UV CD spectra of the disulfide-oxidized monomers can be seen in Fig. 2b. In contrast with disulfide-reduced proteins, all variants exhibit well-folded CD spectra similar to that of WT mAS-SOD1$^{SS}_{Apo}$. Nevertheless, the characteristic shoulder at 230 nm is diminished for A4V, L38V, L106V, and G93A, suggesting some structural differences may exist between these variants and WT mAS-SOD1$^{SS}_{Apo}$.

The stabilities of the disulfide-oxidized and metal-free variants were measured by both kinetic and equilibrium methods. These complementary approaches toward stability measurement are possible because both kinetic and equilibrium mechanisms are well described by two-state processes. The equilibrium urea denaturation curves for mAS-SOD1$^{SS}_{Apo}$ variants at 20 °C and pH 7.2 and the fraction of unfolded plots for these titrations are shown in Fig. 2d and f, respectively. WT and S134N mAS-SOD1$^{SS}_{Apo}$ are stable to ~1.8 M urea, where both proteins undergo a cooperative unfolding reaction that is complete by ~3.8 M urea. The next most stable variant, A4V, undergoes a cooperative unfolding reaction beginning around 0.8 M urea and is complete by 2.8 M urea. L38V, G93A, and L106V variants exhibit sloped native baselines and are completely unfolded by 2 M urea. These equilibrium data were fit to a two-state model as described for the mAS-SOD1$^{SS}_{Apo}$ titrations, except no constraints were imposed on the thermodynamic parameters or baselines and CD spectra between 215 and 245 nm were fit. From the calculated stabilities (Table 1) and the fraction of unfolded plots (Fig. 2f), it is evident that all disulfide-oxidized variants are at least 95% folded at 20 °C and pH 7.2.

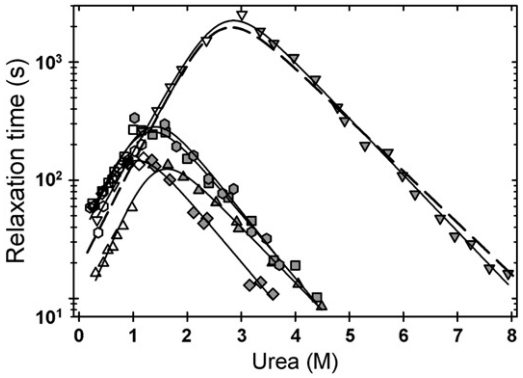

Fig. 5. Observed refolding (open symbols) and unfolding (filled symbols) relaxation times of mAS-SOD1$^{SS}_{Apo}$ variants monitored by CD at 230 nm, at pH 7.2 and 20 °C, and plotted as a function of final denaturant concentration. The data for A4V (triangle), L38V (hexagon), G93A (diamond), L106V (square), and S134N (upside-down triangle) are shown with the best-fit line to a two-state folding reaction (continuous lines). The fit to the disulfide-oxidized WT data (dashed line) was adapted from Svensson *et al.*[16] The buffer used was 10 mM KPi, 1 mM EDTA (pH 7.2).

The stabilities of the mAS-SOD1$^{SS}_{Apo}$ variants were also measured kinetically in order to facilitate an appropriate comparison with the Zn-bound data (see below). The kinetic unfolding and refolding reactions of the mAS-SOD1$^{SS}_{Apo}$ ALS variants at 20 °C and pH 7.2 were monitored by far-UV CD at 230 nm. Both reactions were well described by single exponentials. Semilog plots of the relaxation times as a function of the final denaturant concentration, that is, chevron plots, are shown in Fig. 5. The rate constants for the global unfolding and refolding reactions in the absence of denaturant were obtained by linear extrapolation of the exponentially dependent regions of the chevron plots and calculated by the reciprocal of the relaxation times, $k=1/\tau$. The refolding rates only vary by a factor of 5 from the slowest, G93A, with a rate constant of 0.029 s^{-1}, to the fastest, A4V, with a rate constant of 0.15 s^{-1}. The largest perturbations are observed in the unfolding rates, ranging from 168-fold faster for G93A to 1.7-fold faster for S134N (Table 1), closely paralleling the perturbation in stability for each variant.

The free energy of folding for each variant, determined from the extrapolated rates, $\Delta G^\circ = -RT \ln(k_f/k_u)$, is in very good agreement with the free energy of folding determined from the equilibrium titrations (Table 1). The observed change in stability ranges from no significant difference for S134N to as large as a 2.76 kcal mol^{-1} destabilization for G93A by the kinetic measurement (Table 1).

The effect of ALS mutations on the apparent Zn affinity of mAS-SOD1

The apparent Zn affinity of mAS-SOD1$^{SS}_{Apo}$ variants was determined from the difference in the free energies of their Zn-bound and Zn-free forms relative to the Zn-free unfolded state. Accurate estimates of the stability of the mAS-SOD1$^{SS}_{Zn}$ species cannot be obtained from equilibrium titrations because Zn appears to scramble to the Cu site in the unfolding transition zone.[30] Alternatively, the equilibrium constant for the reversible unfolding reaction can be calculated from the ratio of the rate constants of unfolding and refolding reactions for the zinc-bound unfolded state and the zinc-bound folded state. When combined with the affinity of Zn for the unfolded protein, estimated from a peptide model of the Zn-binding loop,[30] the free energy of Zn binding ($\Delta\Delta G^\circ_{Zn}$), and the corresponding apparent Zn affinity, can be obtained from the difference in the metal-bound (ΔG°_{Zn}) and the metal-free stability(ΔG°_{Apo}): $\Delta\Delta G^\circ_{Zn} = \Delta G^\circ_{Zn}$(Gdn-HCl) $- \Delta G^\circ_{Apo}$(urea), where $\Delta\Delta G^\circ_{Zn} = -RT \ln(K_d)$ (see Kayatekin *et al.*[30] for a detailed explanation of the analysis).

The unfolding and refolding reactions of 10 μM protein loaded with stoichiometric Zn at 20 °C and pH 7.2 were monitored by far-UV CD at 230 nm. Guanidine hydrochloride (Gdn-HCl) rather than urea was used as a denaturant to sample the entire folding reaction coordinate because Zn greatly enhances the stability of SOD1 and requires a more potent denaturant to access the unfolded state. The presence of Zn also required a Hepes buffer because $Zn_3(PO_4)_2$ precipitates at millimolar buffer concentrations. The requirement to change both the denaturant and the buffer to make this comparison means that the dissociation constants should be considered apparent and not absolute. However, because the WT and ALS variants were subjected to the same procedures, the *differences* in the Zn-binding free energies are expected to reflect the inherent differences in affinities induced by the mutations.

Above stoichiometric Zn–protein concentrations for all variants, the refolding reactions were well described by a single exponential phase, corresponding to the faster of the two observed relaxation times at stoichiometric or lower Zn concentrations. The slower reaction corresponds to the folding of mAS-SOD1$^{SS}_{Apo}$.[30] The unfolding reactions displayed a second, faster exponential in the transition zone that has previously been attributed to the scrambling of the Zn ion to the Cu site.[30] The chevron plots for A4V, L38V, and WT mAS-SOD1$^{SS}_{Zn}$ are shown in Fig. 6a, and the chevron plots for G93A, L106V, and S134N are shown in Fig. 6b.

The refolding relaxation times increase exponentially with increasing denaturant concentration to a maximum around 1.8–2.2 M Gdn-HCl. At higher denaturant concentrations the unfolding reaction is favored and the observed unfolding relaxation times decrease exponentially with increasing denaturant concentration. Above 4–5 M Gdn-HCl, the unfolding relaxation times in the presence of Zn for WT mAS-SOD1$^{SS}_{Zn}$ and all of the variants except for L38V roll over to become nearly independent of the

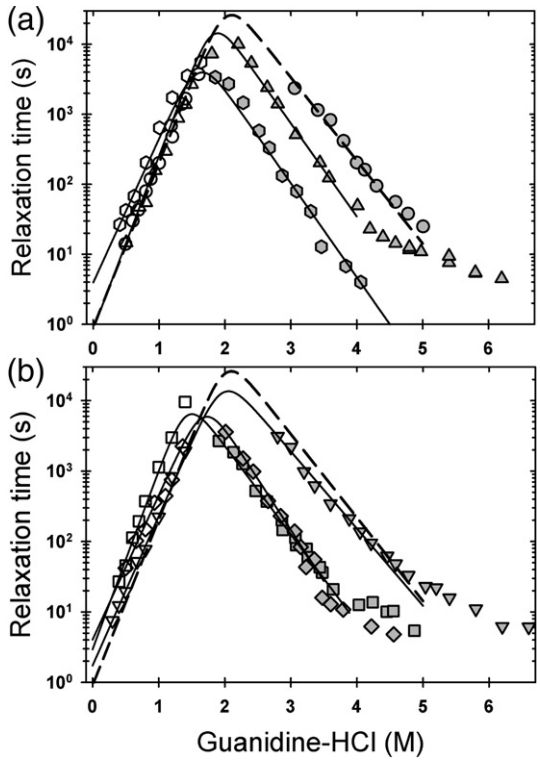

Fig. 6. Observed refolding (open symbols) and unfolding (filled symbols) relaxation times monitored by CD at 230 nm, at pH 7.2 and 20 °C, and plotted as a function of final denaturant concentration. (a) The data for mAS-SOD1$^{SS}_{Zn}$ WT (circle), A4V (triangle), and L38V (hexagon) and (b) the data for mAS-SOD1$^{SS}_{Zn}$ G93A (diamond), L106V (square), and S134N (upside-down triangle) are shown with the best-fit line to a two-state folding reaction. The WT mAS-SOD1$^{SS}_{Zn}$ data were adapted from Kayatekin *et al.*[30] The concentration of protein and Zn for all ALS variants was 10 μM and the buffer used was 20 mM Hepes (pH 7.2).

denaturant concentration. The L38V variant may roll over at fast unfolding rates that are within the dead time of a manual-mixing experiment. These data suggest either that Zn has introduced a rate-limiting rearrangement reaction in the native conformation or that Zn has slowed a rearrangement reaction that was previously undetectable for the apoprotein with manual-mixing techniques. Because this reaction is not kinetically coupled to the major unfolding reaction that controls unfolding above 4–5 M Gdn-HCl, its presence does not interfere with the kinetic measurement of stability.

The refolding rate constants of all the proteins are within a factor of ~5 of each other, ranging from 0.19±0.05 s^{-1} for G93A to 0.74±0.01 s^{-1} for WT to 0.87±0.15 s^{-1} for A4V mAS-SOD1$^{SS}_{Zn}$ (Table 1). The effects of the mutations are substantially greater on the unfolding rate constants, which parallel the effects on stability. WT mAS-SOD1$^{SS}_{Zn}$ is the slowest to unfold, with a rate constant of $0.23\pm0.08\times10^{-7}$ s^{-1}, while L106V unfolds the most rapidly, roughly 60-fold faster, with a rate constant of $13.3\pm3.9\times10^{-7}$ s^{-1}.

These data can be compared with the stabilities of the Zn-free forms of these proteins to yield an apparent Zn affinity for the ALS variants (Table 1). A4V and G93A variants bind Zn slightly tighter than does WT mAS-SOD1^{SS}, while L38V, L106V, and S134N bind Zn more weakly than does the WT protein. The corresponding dissociation constants, K_d, for A4V, L38V, G93A, and L106V are within a factor of 3 of the K_d for WT, 100 pM, and, with the exception of S134N, are nearly within the estimated errors of the measurement. The apparent Zn affinity of S134N is reduced by roughly an order of magnitude compared to WT. Contrasting with the dramatic effects on stability with the loss of the disulfide bond, Zn has little differential effect on the standard-state stability of the A4V, L38V, G93A, and L106V variants. Only the apparent Zn affinity of S134N is significantly reduced from WT mAS-SOD1^{SS}.

The apparent Zn affinity of the disulfide-reduced protein is greatly decreased

The thermodynamic coupling between the disulfide bond and Zn binding was assessed by measuring the Zn affinity of WT and S134N mAS-SOD1^{2SH} with the kinetic assay described above for the mAS-SOD^{ss} species. The chevron plots of WT and S134N mAS-SOD1$^{2SH}_{Apo}$ are shown in Fig. 7a. In both refolding and unfolding, only a single exponential phase was observed. Neither the denaturant dependence of the refolding rate nor the unfolding rate is significantly affected by the loss of the disulfide bond. Both variants exhibit an identical response to disulfide-bond reduction, where the refolding rates are slowed ~3-fold compared to that of the disulfide-oxidized protein and the unfolding rate is accelerated ~5-fold (Table 2).

When Zn was introduced, two phases were observed in refolding and unfolding, comparable to that of the disulfide-oxidized protein. The slower phase in refolding matched the refolding rate of the metal-free protein. The chevron plots of the slow exponential phase in unfolding and the fast phase in refolding at stoichiometric Zn concentrations for WT and S134N mAS-SOD1$^{2SH}_{Zn}$ are shown in Fig. 7b and the associated thermodynamic and kinetics parameters are reported in Table 2. Although the status of the disulfide bond does not alter the denaturant dependence of the refolding reaction, the denaturant dependence of the unfolding reaction is substantially decreased when the disulfide bond is reduced. This change presumably reflects a less structured native state for mAS-SOD1$^{2SH}_{Zn}$ compared to mAS-SOD1$^{SS}_{Zn}$. The refolding rate in the absence of denaturant for WT mAS-SOD1$^{2SH}_{Zn}$ is nearly 10-fold slower than for mAS-SOD1$^{SS}_{Zn}$, while the unfolding rate constant is nearly 1000-fold faster.

Surprisingly, the disulfide-reduced S134N variant clearly exhibits an ~3-fold slower unfolding rate than the WT protein in the presence of Zn, while the refolding rates for both proteins are comparable.

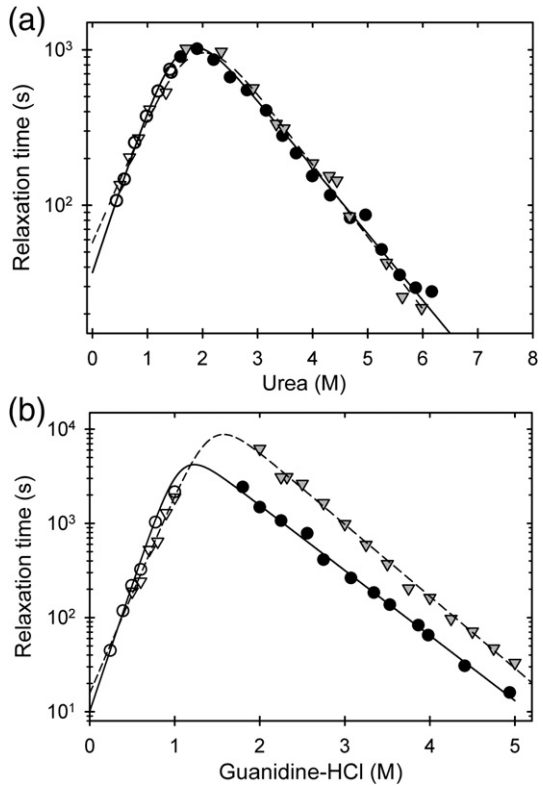

Fig. 7. Observed refolding (open symbols) and unfolding (filled symbols) relaxation times of WT (circles) and S134N (upside-down triangle) (a) mAS-SOD1$^{2SH}_{Apo}$ and (b) mAS-SOD1$^{2SH}_{Zn}$ monitored by CD at 230 nm, at pH 7.2 and 20 °C, and plotted as a function of final denaturant concentration. The data are shown with the best-fit line to a two-state folding reaction for WT (continuous line) and S134N (dashed line). The protein and Zn concentrations were 10 μM and the buffer used was 20 mM Hepes, 1 mM TCEP (pH 7.2).

This result suggests that the replacement of serine with asparagine in the electrostatic loop may actually lead to interactions that stabilize Zn binding compared to the WT protein when the disulfide bond is reduced and the protein relaxes (see Discussion).

Discussion

Patients with the five ALS variants of SOD1 examined in this study, A4V, L38V, G93A, L106V, and S134N, exhibit an average life expectancy of less than 3 years after the onset of disease.[31] Our approach toward testing the potential role of monomeric species in the aggregation hypothesis for toxicity in SOD1-mediated familial ALS has been to employ classical thermodynamic and kinetic folding experiments to define the folding free-energy surface of stable monomeric versions of these variants. The coupling between mutations, disulfide-bond status, and Zn binding can be related to the changes in the relative populations of the folded and unfolded states (Fig. 8). Enhanced populations of marginally soluble monomeric forms would be expected to increase the propensity for aggregation and, possibly, promote toxicity.

Disulfide-reduced ALS variants are very unstable

The reduction of the disulfide bond in the stable monomeric models of the A4V, L38V, G93A, and L106V variants causes a significant reduction in their stability (Table 1) and a corresponding increase in the population of their unfolded states (Fig. 8). For example, G93A mAS-SOD1$^{SS}_{Apo}$, the least stable variant, is only 5% unfolded at 20 °C. Upon reduction of the disulfide bond, the population of unfolded protein increases to 55%. The effect is exacerbated at 37 °C, where the unfolded populations of A4V, L38V, G93A, and L106V exceed 50%, while only 3% of the WT protein is unfolded under these conditions. These results demonstrate that unfolded mAS-SOD1$^{2SH}_{Apo}$ is prevalent in these ALS variants under physiological conditions and, therefore, could play a critical role in aggregation. A recent report has demonstrated that even WT-SOD1$_{Apo}$ can aggregate under conditions that enhance the unfolded state, such as the addition of reducing agent or the presence of 1 M Gdn-HCl, when agitated at 37 °C.[32] Given that the unfolded thermodynamic state represents a manifold of rapidly interconverting conformations, it is also

Table 2. Thermodynamic parameters, microscopic rate constants, and kinetic $m^{\ddagger}$ values for disulfide-reduced WT and S134N

	WT$_{apo}$[a]	S134N$_{apo}$[a]	WT$_{Zn}$[b]	S134N$_{Zn}$[b]
k_f	0.027±0.006	0.019±0.003	0.099±0.005	0.064±0.014
$m^{\ddagger}_f$	1.43±0.23	1.19±0.12	3.6±0.1	2.87±0.17
k_u	(1.0±0.3)×10^{-4}	(6.6±1.7)×10^{-5}	(2.7±0.5)×10^{-5}	(5.2±0.6)×10^{-6}
$m^{\ddagger}_u$	−0.57±0.03	−0.65±0.03	−0.92±0.03	−1.04±0.02
$\Delta G°_{(U/M)}$	3.26±0.22	3.30±0.18	4.78±0.11	5.48±0.14
$m_{(U/M)}$[c]	2.00±0.23	1.84±0.12	4.52±0.1	3.91±0.17
$\Delta G°_{Zn}$	—	—	9.52±0.25	10.2±0.2
K_d[d]	—	—	75±33 nM	25±10 nM

Units for the U⇆M reaction: k_f and k_u, s^{-1}; $m^{\ddagger}_f$, $m^{\ddagger}_u$, and $m_{(U/M)}$, kcal mol^{-1} M^{-1}; $\Delta G°_{(U/M)}$, $\Delta G°_{Zn}$, kcal mol^{-1}.

[a] Denaturation was performed with urea.

[b] Denaturation was performed with Gdn-HCl.

[c] Calculated according to $m_{tot} = /m^{\ddagger}_u/ + /m^{\ddagger}_f/$.

[d] The free-energy difference between U+Zn⇆N•Zn and the Zn affinity was calculated as described in Kayatekin *et al.*[30]

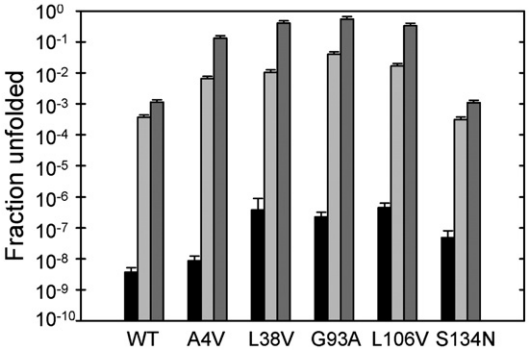

Fig. 8. The fraction of unfolded species populated at equilibrium for each variant, mAS-SOD1$^{SS}_{Zn}$ (black), mAS-SOD1$^{SS}_{Apo}$ (light gray), and mAS-SOD1$^{2SH}_{Apo}$ (dark gray) at 10 μM protein concentration, 20 °C, and pH 7.2. The errors for A4V, L38V, G93A, and L106V mAS-SOD1$^{2SH}_{Apo}$ were approximated at 20%. All other errors were determined from the error in the $\Delta G°$.

possible that a transient population of substructure might be more aggregation-prone and, therefore, responsible for the initiation of the aggregation reaction.

Implications for mitochondrial damage

The dramatic destabilization of the disulfide-reduced forms of the A4V, L38V, G93A, and L106V variants may also play a role in mitochondrial damage observed in mouse models of ALS.[33] The transport of SOD1 into yeast mitochondria is greatly favored for the reduced metal-free monomeric form,[34] presumably reflecting the ease of access to an unstructured unfolded state required to traverse the outer membrane. Once inside the intermembrane space, a resident disulfide relay system oxidizes the intramolecular disulfide bond, which, along with Zn binding and dimer formation, would effectively trap SOD1 inside the mitochondria.[35] The dominant population of the unfolded state for the disulfide-reduced form of the four WT-like variants, A4V, L38V, G93A, and L106V, at pH 7.2 and 37 °C and the unusually slow folding reaction to the disulfide-competent folded state could provide an opportunity for the unfolded state to aggregate or to associate with other components in the intermembrane space. The observed increased localization of G93A and other ALS variants of SOD1 in mitochondria,[36] especially in the spinal cord of transgenic mice,[37] and their capacity to damage this essential organelle may, therefore, be a manifestation of their thermodynamic and kinetic folding properties.

Zn binding is marginally affected in WT-like ALS variants

NMR and crystallographic studies have shown that Zn binding has an important role in defining the structure of SOD1 by organizing the Zn binding and electrostatic loops of the WT protein.[25,26,38] As shown in the present study, Zn binding to mAS-SOD1^{SS} significantly stabilizes the folded state for all of the variants (Table 1). However, the apparent dissociation constants for the WT-like variants, A4V, L38V, G93A, and L106V, vary by less than an order of magnitude from the 100 pM apparent K_d for the WT protein and are not consistently decreased. Despite the small differences in the measured Zn affinity, these results correlate well with the observed metal content of the mutant protein when isolated from insect cells.[39]

These results may appear to contradict the findings by Crow *et al.*,[40] who found that the dimeric A4V and L38V SOD1 variants had a 30- and 18-fold weakening of the Zn affinity relative to that of WT protein in 2 M urea; the contradiction can be understood in terms of the increased population of the folded monomeric forms for these variants and their lower zinc affinity relative to the that of the dimeric state.[30] The 66 h required to extract zinc from these variants in the Crow *et al.* study would provide ample opportunity for the monomeric form to serve as the conduit for zinc loss.

S134N, a metal-binding variant of SOD1, differs from the β-sandwich variants in that the apparent Zn affinity is significantly reduced. While the S134N variant is not destabilized significantly in its metal-free forms, the weakening in the apparent K_d for Zn binding from 100 pM for WT mAS-SOD1^{SS} to 1.6 nM for S134N mAS-SOD1^{SS} offers the possibility that aggregation of the monomeric forms may still be the source of toxicity. Although this variant can be loaded with Zn and Cu *in vitro*,[41,42] Hayward and coworkers[43] have observed decreased Zn and Cu content in as-isolated samples of S134N SOD1 expressed in insect cells. The replacement of serine with asparagine in the electrostatic loop may similarly impede full metallation in motor neurons. The potential for aggregation might be further compounded by the spontaneous reduction of the disulfide bond of the metal-free species in the cytoplasm. Thus, even the small fraction of unfolded mAS-SOD1^{2SH} observed for S134N may be sufficient to cause aggregation. Because the predicted metal-free unfolded and folded populations for S134N are nearly identical to WT, the intriguing possibility arises that the loss of Zn even from the WT protein may be sufficient to trigger aggregation.

Zn binding is dramatically decreased by reduction of the disulfide bond

In contrast to the response to mutations, the reduction of the disulfide bond has a dramatic effect on the Zn affinity of mAS-SOD1, resulting in a ~750-fold weakening in the apparent K_d from 100 pM to 75 nM for the WT protein and a 16-fold weakening in the apparent K_d for the S134N variant from 1.6 to 25 nM. The 3-fold tighter K_d for disulfide-reduced S134N *versus* WT protein contrasts with a 16-fold weaker apparent K_d in the presence of the disulfide bond. This behavior

demonstrates thermodynamic coupling between the disulfide bond and Zn binding. Inspection of the crystal structure of SOD1 shows that the disulfide bond is proximal to the Cu site, which shares a ligand with the Zn site. Apparently, the constraints on the structure introduced by the disulfide bond are transmitted to the Zn binding site in a way that reduces the affinity of S134N for Zn. This may be due to the inability of the S134N variant to induce compactness in the electrostatic loop by the formation of the S134–D125 hydrogen bond.[41] When the protein relaxes in the absence of the disulfide bond, the electrostatic loop may be able to access conformers that form stabilizing electrostatic interactions absent in the WT protein.

These results suggest that disulfide bond oxidation may be the key step in the maturation of SOD1. Because $SOD1^{2SH}_{Apo}$ would not compete effectively for free Zn at ~1 nM concentration *in vivo*, Zn would be expected to bind after the oxidation of the disulfide bond when the apparent K_d decreases to 100 pM. This hypothesis is supported by the discovery that the presence of Zn does not accelerate the formation of the disulfide bond in SOD1 expressed in rabbit reticulocyte assays.[44]

Aggregation following synthesis on the ribosome?

The analysis presented above presumes that the populations of species *in vivo* dictated by the equilibrium free-energy surface of SOD1 are those responsible for aggregation and toxicity. Alternately, the aggregation of SOD1 may occur soon after synthesis on the ribosome, prior to its several maturation steps including disulfide bond formation, dimerization, and Zn and Cu loading.[44] Disulfide-reduced SOD1 folds surprisingly slowly *in vitro*, requiring ~40 s at 20 °C, nearly 4 orders of magnitude slower than predicted by its topology.[45] Although the time required for folding is comparable to the length of time required to translate a 153-residue eukaryotic protein, ~30–50 s,[46] cotranslational folding of SOD1 is unlikely, since the rate-limiting step of folding involves the docking of the first four N-terminal β-strands with the β7 strand near the C-terminus.[47] The observation that the four ALS variants in the β-sandwich structure, A4V, L38V, G93A, and L106V, have substantially increased unfolded populations of their disulfide-reduced forms implies an enhanced opportunity for the aggregation of these species prior to their ultimate maturation to their native dimeric forms. The subsequent formation of the disulfide bond increases the stability of the folded monomeric form and drives the dimerization reaction.[21] The high concentration of SOD1 in motor neurons, >10 μM,[9] and its half-life of ~1 day,[48] requires a constant and significant rate of synthesis on ribosomes. Thus, the aggregation of SOD1 may involve both kinetic, that is, following synthesis and prior to maturation, and thermodynamic, that is, at steady state after maturation,[20] mechanisms.

Materials and Methods

Protein purification

Recombinant proteins were expressed in and purified from BL21-Gold(DE3) PLysS cells (Stratagene®, Inc. Cedar Creek, TX). The protein was purified using the procedure previously described in Kayatekin *et al.*[30] Protein identity and purity were determined by measuring the molecular weight with liquid chromatography–electrospray ionization mass spectrometry. The protein concentrations were calculated using an extinction coefficient of 5400 M^{-1} cm^{-1}.

Disulfide-bond reduction

All variants of mAS-SOD were reduced by 24-h incubation in 1 mM TCEP [tris(2-carboxyethyl)phosphine]. The reduction of the disulfide bond and absence of reoxidation after the incubation in reducing agent was confirmed by kinetic unfolding or refolding experiments for mAS-$SOD1_{Apo}$. Fully reduced protein exhibited a single exponential phase with a relaxation time fivefold faster than that of the disulfide-oxidized protein in unfolding.

Equilibrium experiments

All CD spectroscopy was performed on a Jasco-810 spectropolarimeter (Jasco Inc., Easton, MD) equipped with a water-cooled Peltier temperature-control system. The CD spectra of disulfide-reduced protein were an average of six spectra obtained using a 1 -mm path length quartz cuvette, a scan rate of 20 nm min^{-1}, and a response time of 4 s. The buffer used was 10 mM potassium phosphate (KPi), 1 mM ethylenediaminetetraacetic acid (EDTA), 1 mM TCEP (pH 7.2). The urea-induced unfolding curves were monitored from 220 to 240 nm in a 0.5 -cm path length quartz cuvette using a scan rate of 20 nm min^{-1} and a response time of 8 s. The buffer used was 20 mM Hepes, 1 mM EDTA, 1 mM TCEP for disulfide-reduced and 10 mM KPi, and 1 mM EDTA for disulfide-oxidized samples (pH 7.2). Urea concentrations were determined by refractive index on a Leica Mark II refractometer. Titration samples were made from concentration-matched stocks of folded protein in standard buffer and unfolded protein at 8 M urea and incubated at the experimental temperature overnight.

Kinetic experiments

The unfolding and refolding kinetics, initiated by manual mixing, were monitored by CD. For metal-free protein, the buffer was 10 mM potassium phosphate and 1 mM EDTA (pH 7.2). For metal-bound protein the potassium phosphate was replaced with 20 mM Hepes and the 1 mM EDTA was omitted. Data were collected at 230 nm in a 1 -cm^2 cuvette under continuous mixing with a solution volume of 1.9 mL. Unfolding jumps were initiated from protein in 0 M urea or Gdn-HCl and refolding jumps were initiated from protein denatured in 4–6 M Gdn-HCl or 8 M urea to various final concentrations. For Zn-loaded samples, the protein was incubated with stoichiometric Zn prior to dilution in the unfolding/refolding buffer. The final concentration of Gdn-HCl was measured by index of refraction. Protein concentrations were 10 μM for all kinetic experiments.

Acknowledgements

We thank Dr. Osman Bilsel, Sagar V. Kathuria, Steven F. Trueman, and Ian M. Love for many helpful discussions; Nicole Washington for purifying S134N mAS-SOD1; and Jessica Adefusika, Graham Dobereiner, and Matt Samberg for creating the bacterial constructs. This work was supported by National Institutes of Health grant GM54836; support for mass spectrometry was provided by NICHD IDDRC Core Grant HD04147.

References

1. Rowland, L. P. & Shneider, N. A. (2001). Amyotrophic lateral sclerosis. *N. Engl. J. Med.* **344**, 1688–1700.
2. Rosen, D. R., Siddique, T., Patterson, D., Figlewicz, D. A., Sapp, P., Hentati, A. *et al.* (1993). Mutations in Cu/Zn superoxide dismutase gene are associated with familial amyotrophic lateral sclerosis. *Nature*, **362**, 59–62.
3. Andersen, P. M., Sims, K. B., Xin, W. W., Kiely, R., O'Neill, G., Ravits, J. *et al.* (2003). Sixteen novel mutations in the Cu/Zn superoxide dismutase gene in amyotrophic lateral sclerosis: a decade of discoveries, defects and disputes. *Amyotrophic Lateral Scler. Other Motor Neuron Disord.* **4**, 62–73.
4. Bruijn, L. I., Houseweart, M. K., Kato, S., Anderson, K. L., Anderson, S. D., Ohama, E. *et al.* (1998). Aggregation and motor neuron toxicity of an ALS-linked SOD1 mutant independent from wild-type SOD1. *Science*, **281**, 1851–1854.
5. Valentine, J. S., Doucette, P. A. & Zittin Potter, S. (2005). Copper-zinc superoxide dismutase and amyotrophic lateral sclerosis. *Annu. Rev. Biochem.* **74**, 563–593.
6. Ross, C. A. & Poirier, M. A. (2004). Protein aggregation and neurodegenerative disease. *Nat. Med.* **10**(Suppl.), S10–S17.
7. McCord, J. M. & Fridovich, I. (1969). Superoxide dismutase. An enzymic function for erythrocuprein (hemocuprein). *J. Biol. Chem.* **244**, 6049–6055.
8. Seetharaman, S. V., Prudencio, M., Karch, C., Holloway, S. P., Borchelt, D. R. & Hart, P. J. (2009). Immature copper-zinc superoxide dismutase and familial amyotrophic lateral sclerosis. *Exp. Biol. Med. (Maywood)*, **234**, 1140–1154.
9. Rakhit, R., Crow, J. P., Lepock, J. R., Kondejewski, L. H., Cashman, N. R. & Chakrabartty, A. (2004). Monomeric Cu,Zn-superoxide dismutase is a common misfolding intermediate in the oxidation models of sporadic and familial amyotrophic lateral sclerosis. *J. Biol. Chem.* **279**, 15499–15504.
10. Rakhit, R., Robertson, J., Vande Velde, C., Horne, P., Ruth, D. M., Griffin, J. *et al.* (2007). An immunological epitope selective for pathological monomer-misfolded SOD1 in ALS. *Nat. Med.* **13**, 754–759.
11. Hough, M. A., Grossmann, J. G., Antonyuk, S. V., Strange, R. W., Doucette, P. A., Rodriguez, J. A. *et al.* (2004). Dimer destabilization in superoxide dismutase may result in disease-causing properties: structures of motor neuron disease mutants. *Proc. Natl Acad. Sci. USA*, **101**, 5976–5981.
12. Zetterstrom, P., Stewart, H. G., Bergemalm, D., Jonsson, P. A., Graffmo, K. S., Andersen, P. M. *et al.* (2007). Soluble misfolded subfractions of mutant superoxide dismutase-1s are enriched in spinal cords throughout life in murine ALS models. *Proc. Natl Acad. Sci. USA*, **104**, 14157–14162.
13. Caughey, B. & Lansbury, P. T. (2003). Protofibrils, pores, fibrils, and neurodegeneration: separating the responsible protein aggregates from the innocent bystanders. *Annu. Rev. Neurosci.* **26**, 267–298.
14. Stefani, M. & Dobson, C. M. (2003). Protein aggregation and aggregate toxicity: new insights into protein folding, misfolding diseases and biological evolution. *J. Mol. Med.* **81**, 678–699.
15. Teilum, K., Smith, M. H., Schulz, E., Christensen, L. C., Solomentsev, G., Oliveberg, M. & Akke, M. (2009). Transient structural distortion of metal-free Cu/Zn superoxide dismutase triggers aberrant oligomerization. *Proc. Natl Acad. Sci. USA*, **106**, 18273–18278.
16. Svensson, A. K., Bilsel, O., Kondrashkina, E., Zitzewitz, J. A. & Matthews, C. R. (2006). Mapping the folding free energy surface for metal-free human Cu,Zn superoxide dismutase. *J. Mol. Biol.* **364**, 1084–1102.
17. Lindberg, M. J., Normark, J., Holmgren, A. & Oliveberg, M. (2004). Folding of human superoxide dismutase: disulfide reduction prevents dimerization and produces marginally stable monomers. *Proc. Natl Acad. Sci. USA*, **101**, 15893–15898.
18. Lindberg, M. J., Tibell, L. & Oliveberg, M. (2002). Common denominator of Cu/Zn superoxide dismutase mutants associated with amyotrophic lateral sclerosis: decreased stability of the apo state. *Proc. Natl. Acad. Sci. USA*, **99**, 16607–16612.
19. Vassall, K. A., Stathopulos, P. B., Rumfeldt, J. A., Lepock, J. R. & Meiering, E. M. (2006). Equilibrium thermodynamic analysis of amyotrophic lateral sclerosis-associated mutant apo Cu,Zn superoxide dismutases. *Biochemistry*, **45**, 7366–7379.
20. Svensson, A. K., Bilsel, O., Kayatekin, C., Adefusika, J. A., Zitzewitz, J. A. & Matthews, C. R. (2010). Metal-free ALS-variants of dimeric human Cu,Zn-superoxide dismutase have enhanced populations of monomeric species. *PLoS One*. In press. doi:10.1371/journal.pone.0010064.
21. Arnesano, F., Banci, L., Bertini, I., Martinelli, M., Furukawa, Y. & O'Halloran, T. V. (2004). The unusually stable quaternary structure of human Cu, Zn-superoxide dismutase 1 is controlled by both metal occupancy and disulfide status. *J. Biol. Chem.* **279**, 47998–48003.
22. Furukawa, Y. & O'Halloran, T. V. (2005). Amyotrophic lateral sclerosis mutations have the greatest destabilizing effect on the apo- and reduced form of SOD1, leading to unfolding and oxidative aggregation. *J. Biol. Chem.* **280**, 17266–17274.
23. Bertini, I., Piccioli, M., Viezzoli, M. S., Chiu, C. Y. & Mullenbach, G. T. (1994). A spectroscopic characterization of a monomeric analog of copper, zinc superoxide dismutase. *Eur. Biophys. J.* **23**, 167–176.
24. Hallewell, R. A., Imlay, K. C., Lee, P., Fong, N. M., Gallegos, C., Getzoff, E. D. *et al.* (1991). Thermostabilization of recombinant human and bovine CuZn superoxide dismutases by replacement of free cysteines. *Biochem. Biophys. Res. Commun.* **181**, 474–480.
25. Banci, L., Bertini, I., Cantini, F., D'Onofrio, M. & Viezzoli, M. S. (2002). Structure and dynamics of copper-free SOD: the protein before binding copper. *Protein Sci.* **11**, 2479–2492.
26. Strange, R. W., Antonyuk, S., Hough, M. A., Doucette, P. A., Rodriguez, J. A., Hart, P. J. *et al.* (2003). The structure of holo and metal-deficient wild-type human Cu, Zn superoxide dismutase and its relevance to

familial amyotrophic lateral sclerosis. *J. Mol. Biol.* **328**, 877–891.
27. Stathopulos, P. B., Rumfeldt, J. A., Karbassi, F., Siddall, C. A., Lepock, J. R. & Meiering, E. M. (2006). Calorimetric analysis of thermodynamic stability and aggregation for apo and holo amyotrophic lateral sclerosis-associated Gly-93 mutants of superoxide dismutase. *J. Biol. Chem.* **281**, 6184–6193.
28. Ionescu, R. M., Smith, V. F., O'Neill, J. C., Jr. & Matthews, C. R. (2000). Multistate equilibrium unfolding of *Escherichia coli* dihydrofolate reductase: thermodynamic and spectroscopic description of the native, intermediate, and unfolded ensembles. *Biochemistry*, **39**, 9540–9550.
29. Shaw, B. F., Durazo, A., Nersissian, A. M., Whitelegge, J. P., Faull, K. F. & Valentine, J. S. (2006). Local unfolding in a destabilized, pathogenic variant of superoxide dismutase 1 observed with H/D exchange and mass spectrometry. *J. Biol. Chem.* **281**, 18167–18176.
30. Kayatekin, C., Zitzewitz, J. A. & Matthews, C. R. (2008). Zinc binding modulates the entire folding free energy surface of human Cu,Zn superoxide dismutase. *J. Mol. Biol.* **384**, 540–555.
31. Wang, Q., Johnson, J. L., Agar, N. Y. & Agar, J. N. (2008). Protein aggregation and protein instability govern familial amyotrophic lateral sclerosis patient survival. *PLoS Biol.* **6**, e170.
32. Chattopadhyay, M., Durazo, A., Sohn, S. H., Strong, C. D., Gralla, E. B., Whitelegge, J. P. & Valentine, J. S. (2008). Initiation and elongation in fibrillation of ALS-linked superoxide dismutase. *Proc. Natl Acad. Sci. USA*, **105**, 18663–18668.
33. Hervias, I., Beal, M. F. & Manfredi, G. (2006). Mitochondrial dysfunction and amyotrophic lateral sclerosis. *Muscle Nerve*, **33**, 598–608.
34. Field, L. S., Furukawa, Y., O'Halloran, T. V. & Culotta, V. C. (2003). Factors controlling the uptake of yeast copper/zinc superoxide dismutase into mitochondria. *J. Biol. Chem.* **278**, 28052–28059.
35. Hell, K. (2008). The Erv1-Mia40 disulfide relay system in the intermembrane space of mitochondria. *Biochim. Biophys. Acta*, **1783**, 601–609.
36. Kawamata, H. & Manfredi, G. (2008). Different regulation of wild-type and mutant Cu,Zn superoxide dismutase localization in mammalian mitochondria. *Hum. Mol. Genet.* **17**, 3303–3317.
37. Liu, J., Lillo, C., Jonsson, P. A., Vande Velde, C., Ward, C. M., Miller, T. M. *et al.* (2004). Toxicity of familial ALS-linked SOD1 mutants from selective recruitment to spinal mitochondria. *Neuron*, **43**, 5–17.
38. Banci, L., Bertini, I., Cramaro, F., DelConte, R. & Viezzoli, M. S. (2003). Solution structure of apo Cu,Zn superoxide dismutase: role of metal ions in protein folding. *Biochemistry*, **42**, 9543–9553.
39. Rodriguez, J. A., Valentine, J. S., Eggers, D. K., Roe, J. A., Tiwari, A., Brown, R. H., Jr & Hayward, L. J. (2002). Familial amyotrophic lateral sclerosis-associated mutations decrease the thermal stability of distinctly metallated species of human copper/zinc superoxide dismutase. *J. Biol. Chem.* **277**, 15932–15937.
40. Crow, J. P., Sampson, J. B., Zhuang, Y., Thompson, J. A. & Beckman, J. S. (1997). Decreased zinc affinity of amyotrophic lateral sclerosis-associated superoxide dismutase mutants leads to enhanced catalysis of tyrosine nitration by peroxynitrite. *J. Neurochem.* **69**, 1936–1944.
41. Banci, L., Bertini, I., D'Amelio, N., Gaggelli, E., Libralesso, E., Matecko, I. *et al.* (2005). Fully metallated S134N Cu,Zn-superoxide dismutase displays abnormal mobility and intermolecular contacts in solution. *J. Biol. Chem.* **280**, 35815–35821.
42. Elam, J. S., Taylor, A. B., Strange, R., Antonyuk, S., Doucette, P. A., Rodriguez, J. A. *et al.* (2003). Amyloid-like filaments and water-filled nanotubes formed by SOD1 mutant proteins linked to familial ALS. *Nat. Struct. Biol.* **10**, 461–467.
43. Hayward, L. J., Rodriguez, J. A., Kim, J. W., Tiwari, A., Goto, J. J., Cabelli, D. E. *et al.* (2002). Decreased metallation and activity in subsets of mutant superoxide dismutases associated with familial amyotrophic lateral sclerosis. *J. Biol. Chem.* **277**, 15923–15931.
44. Bruns, C. K. & Kopito, R. R. (2007). Impaired post-translational folding of familial ALS-linked Cu, Zn superoxide dismutase mutants. *EMBO J.* **26**, 855–866.
45. Plaxco, K. W., Simons, K. T. & Baker, D. (1998). Contact order, transition state placement and the refolding rates of single domain proteins. *J. Mol. Biol.* **277**, 985–994.
46. Hershey, J. W. (1991). Translational control in mammalian cells. *Annu. Rev. Biochem.* **60**, 717–755.
47. Nordlund, A. & Oliveberg, M. (2006). Folding of Cu/Zn superoxide dismutase suggests structural hotspots for gain of neurotoxic function in ALS: parallels to precursors in amyloid disease. *Proc. Natl Acad. Sci. USA*, **103**, 10218–10223.
48. Borchelt, D. R., Lee, M. K., Slunt, H. S., Guarnieri, M., Xu, Z. S., Wong, P. C. *et al.* (1994). Superoxide dismutase 1 with mutations linked to familial amyotrophic lateral sclerosis possesses significant activity. *Proc. Natl Acad. Sci. USA*, **91**, 8292–8296.